

Far-infrared spectra of polycrystalline  $\text{Ba}_2\text{YCu}_3\text{O}_{9-\delta}$ 

G. A. Thomas, H. K. Ng,\* A. J. Millis, R. N. Bhatt, R. J. Cava, E. A. Rietman,  
D. W. Johnson, Jr., G. P. Espinosa, and J. M. Vandenberg  
AT&T Bell Laboratories, Murray Hill, New Jersey 07974  
(Received 21 April 1987)

We present far-infrared reflectivity spectra of seven samples of ceramic superconductors in the Ba-Y-Cu-O system with transition temperatures near 93 K. We find superconducting gap structures on the basis of which we estimate the ratio of twice the average gap to the transition temperature to be consistent with 3.5, but possibly higher. Questions of normal-state characterization preclude a definitive analysis.

We have investigated the optical properties of the Ba-Y-Cu-O ceramic system which has been found to exhibit superconductivity near 93 K on both mixed-<sup>1,2</sup> and single-phase<sup>3-5</sup> materials. We have studied the energy range near which structure due to the superconducting energy gap would be expected within the framework of the BCS theory. Our motivation is to try to understand the current materials status of these ceramics, as well as the extent to which a BCS type of analysis<sup>6</sup> is applicable.

Figure 1 shows the reflectivity  $R$  in the normal state of seven ceramic samples (numbered in order to their preparation) all of which are found to exhibit bulk superconductivity below temperatures  $T_c$  of approximately 93 K. The frequency range measured was about 40 to 350  $\text{cm}^{-1}$ . The upper five curves are measurements of pressed

pellets of the composition  $\text{Ba}_2\text{YCu}_3\text{O}_{9-\delta}$ , with  $\delta \approx 2.1$ , and are nominally single phase. The lower two curves in the inset represent the mixed-phase composition  $\text{Y}_{1.2}\text{Ba}_{0.8}\text{CuO}_4$  as a powder and as a pressed pellet.

The variability in the observed behavior indicates that material preparation and handling techniques are in a continuing state of refinement. Nevertheless, we have analyzed the data for our most reflecting sample using the Mattis-Bardeen theory<sup>6</sup> in conjunction with the effective-medium approximation<sup>7</sup> to extract a probable value for the superconducting energy gap. We also compare our results with some other gap measurements.<sup>8,9</sup> Such an analysis should be considered preliminary, and we suggest that a similar caution also applies to recent optical<sup>10-14</sup> and tunneling<sup>15,16</sup> measurements on  $(\text{La,Sr})_2\text{CuO}_4$ .

The single-phase material showing the highest  $R$  was prepared by heating the ground, mixed chemical constituents at 950°C in air for one day, pressing into a pellet, sintering in flowing  $\text{O}_2$  for 16 h, heating in  $\text{O}_2$  at 700°C for 14 h, and cooling to 200°C in  $\text{O}_2$ .

The  $R$  measurements shown were made using a Michelson interferometer, with the light reflected once from the sample at an angle of incidence 15° from normal. The light intensity was detected using a composite bolometer cooled to 0.3 K using charcoal-pumped liquid  $^3\text{He}$ . The intensity was reduced by irises and filters by factors over  $10^3$  from the maximum available to avoid overloading the detector, and a series of measurements was made as a function of light intensity to check detector linearity under the measurement conditions. The samples were held at temperatures  $T$  between 95 and 100 K for all of the measurements shown in Fig. 1, but  $T$  was also varied and controlled over the range 10 to 120 K for other spectra.

The samples labeled 3-6 in Fig. 1 were polished using dry emery paper to take off a thick layer of the pellet and then to produce as smooth a surface as possible. Some pits were present in most samples, but the appearance was otherwise uniform. Curve 5' represents the same sample as curve 5, but measured five days later. The samples were stored in air at room temperature and were each measured initially within about two days of their final heat treatment. The samples from which curves 2 and 3 were obtained were polished using water slurries and were apparently degraded by that process.

The variation among the samples was investigated by

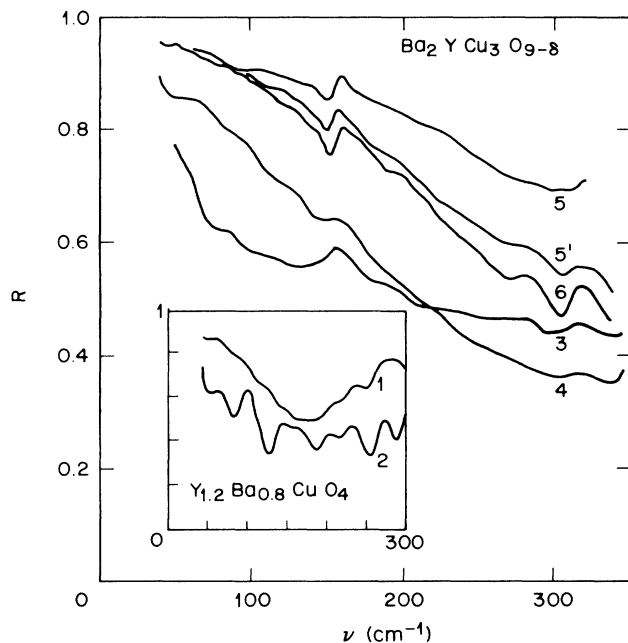


FIG. 1. Seven curves showing the reflectivity  $R$  as a function of frequency  $\nu$  for samples of mixed phase  $\text{Y}_{1.2}\text{Ba}_{0.8}\text{CuO}_4$  [inset, curves 1 (powder) and 2 (pressed pellet)] and single phase  $\text{Ba}_2\text{YCu}_3\text{O}_{9-\delta}$ ,  $\delta \approx 2.1$  [curves 3-6 (pressed pellets)] at temperatures 95 to 100 K, numbered in the order prepared.

x-ray photographic analysis using a high-resolution Huber powder-diffraction camera with monochromatic  $\text{Cu } K\alpha_1$  radiation. The x-ray diffraction pattern showed the presence of unreacted  $\text{BaY}_2\text{O}_4$  in the volume fractions 0.15 for curve 4, 0.05 for curve 6, and  $<0.01$  for curve 5. We suspect that the drop in  $R$  between curves 5 and 5' is due to exposure to water vapor in the laboratory air. The mixed-phase materials have lower  $R$ , as might be expected.

All of the pressed pellet samples were measured in comparison to a polished brass reference which was moved into the light path in place of the sample without changing  $T$ . The powder reflectance (curve 1) was obtained from a sample within a thin, uniform layer of vacuum grease on a wedged sapphire crystal with a strongly absorbing backing, and was compared to a reference that was the same except for the powder. Some Fabry-Perot oscillations are present.

All of the samples shown in Fig. 1 were cooled below  $T_c$  and remeasured. Figure 2 shows a comparison of the spectra at 20 and 100 K,  $R_S$  and  $R_N$ , respectively, for the sample with the highest  $R$ . This sample, curve 5 in Fig. 1, also showed a large  $R_S - R_N$  with a positive maximum of about 5%. Curve 5' showed a 2% peak, with curves 6, 4, and 3 at other values. The mixed-phase materials showed small changes but were not further analyzed. All of the data could be characterized by the same qualitative analysis as for the structure shown in Fig. 2 and suggest similar estimates of the average gap parameter  $2\Delta$ .

The curves in Fig. 2 show three sharp lines at 151, 268, and  $303 \text{ cm}^{-1}$ , with uncertainties  $\pm 1 \text{ cm}^{-1}$ , and full widths at half maximum of  $8 \text{ cm}^{-1}$  which are essentially the same as our spectral resolution of  $7.5 \text{ cm}^{-1}$ . These lines are most likely due to phonons whose contributions to  $R_S$  are enhanced because of the smaller electronic absorption in the superconducting state than in the normal. Weber<sup>17</sup> has calculated that the phonon modes in this frequency range for the  $(\text{La,Sr})_2\text{CuO}_4$  system are due to  $\text{Cu-O}$ ,  $\text{La-O}$ , and  $\text{Sr-O}$  bond bending, and it seems likely that the same types of modes are seen here. Since the phonon resonances in the normal state have shapes with the maximum at higher frequency, the absorption is probably occurring in metallic regions of the sample rather than in insulating inclusions.

The vertical bars on the curve indicate some estimates of the experimental uncertainties in  $R$ , which are largest at the ends of our frequency range because of the small light intensity from our source at low energy and our

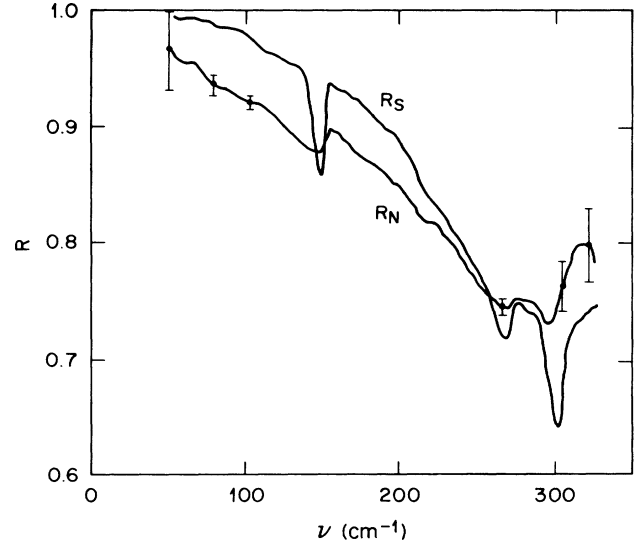


FIG. 2. Expanded view of the spectrum in the normal state  $R_N$  for curve 5 of Fig. 1 and of the same sample in the superconducting state  $R_S$ .

cutoff filters at high energy. There is a clearly defined, broad background difference between the  $R_S$  and  $R_N$  curves in Fig. 2 with a crossing at about  $260 \text{ cm}^{-1}$ . This structure is due to the formation of the superconducting energy gap and is similar to that seen in the  $(\text{La,Sr})_2\text{CuO}_4$  system.<sup>10-14</sup>

To interpret these data, we have computed  $R$  from the usual normal-incidence formula,

$$R = |(\epsilon^{1/2} - 1)/(\epsilon^{1/2} + 1)|^2, \quad (1)$$

where  $\epsilon = 1 + 4\pi i\sigma/\omega$  is the complex, frequency-dependent dielectric function, and  $\sigma = \sigma_1 + i\sigma_2$  is the complex conductivity. For the normal state we have used a Drude model

$$\sigma_N = \sigma_0/(1 - i\omega\tau), \quad (2)$$

where  $\sigma_0$  is the dc conductivity. We have chosen  $\sigma_0 = 1.4 \times 10^{-3} (\mu\Omega \text{ cm})^{-1}$  to reproduce  $R_N$  approximately between 50 and  $100 \text{ cm}^{-1}$ ; this  $\sigma_0$  is about  $\frac{1}{3}$  of the measured dc value, indicating that our understanding of  $R_N$  is incomplete.

To model  $R_S$ , we replace the Drude conductivity by the  $T=0 \text{ K}$ , dirty-limit, Mattis-Bardeen result<sup>6</sup>

$$\sigma_{1S} = (\sigma_0/\tilde{\omega}) \left[ (\tilde{\omega} + 1)E \left[ \frac{\tilde{\omega} - 1}{\tilde{\omega} + 1} \right] - 2K \left[ \frac{\tilde{\omega} - 1}{\tilde{\omega} + 1} \right] \right] \Theta(\tilde{\omega} - 1), \quad (3a)$$

$$\sigma_{2S} = (\sigma_0/2\tilde{\omega}) \left[ (\tilde{\omega} + 1)E \left[ \frac{2\tilde{\omega}^{1/2}}{\tilde{\omega} + 1} \right] - (\tilde{\omega} - 1)K \left[ \frac{2\tilde{\omega}^{1/2}}{\tilde{\omega} + 1} \right] \right], \quad (3b)$$

where  $E$  and  $K$  are complete elliptic integrals,  $\Theta$  is the step function,  $\sigma_S = \sigma_{1S} + i\sigma_{2S}$ , and  $\tilde{\omega} \equiv \omega/2\Delta$ . Equation (3) applies for  $2\Delta \ll 1/\tau$  and  $\omega < 1/\tau$ , where  $1/\tau$  is the scattering rate.

For orientation, Fig. 3(a) illustrates that  $\sigma_{1S}$  is zero for energies below  $2\Delta$  while  $\sigma_{2S}$  diverges as frequency goes to

zero as  $\omega^{-1}$ . With a large, purely imaginary conductivity, light in the energy range  $\tilde{\omega} < 1$  is unattenuated and perfectly reflected, as illustrated in Fig. 3(b). The energy gap in this ideal case can unambiguously be determined from the point at which  $R$  begins to deviate from 1.

This ideal behavior is not seen in Fig. 2; in particular,

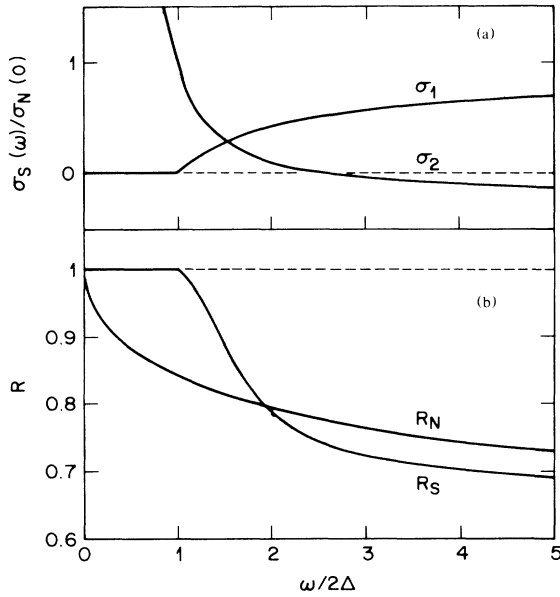


FIG. 3. (a) Real  $\sigma_{1S}$ , and imaginary  $\sigma_{2S}$ , parts of the normalized conductivity in the superconducting state according to Mattis-Bardeen theory as a function of frequency normalized to the optical energy gap  $\omega/2\Delta$ . (b) Theoretical curves for a normal state (Drude) reflectivity  $R_N$  and for a superconducting state (Mattis-Bardeen) reflectivity  $R_S$ .

the reflectivity in the superconducting state is never unity. We believe this nonideal behavior can be modeled approximately by assuming that some fraction  $f$  of the surface region probed by the light does not become superconducting, remaining instead metallic down to our lowest  $T$  (10 K). (We estimate the penetration depth of the light to be  $\sim 10 \mu\text{m}$ .)

To determine the conductivity  $\sigma$  of the normal-superconducting composite, we have used the effective-medium approximation:<sup>7</sup>

$$f \frac{\sigma - \sigma_N}{\sigma + 2\sigma_N} + (1-f) \frac{\sigma - \sigma_S}{\sigma + 2\sigma_S} = 0, \quad (4)$$

where we have chosen the root of this quadratic equation with positive imaginary part and assumed the spherical shape factor 2.

Our model is clearly oversimplified. We feel that a definitive analysis must include effects due to anisotropy in both  $\sigma$  and  $\Delta$ , as well as non-Drude behavior due to resonances (whose effect we find to be strong in the La-Sr material<sup>14</sup>) or "interband transitions," and to the strong inelastic scattering believed to produce the linear variation with  $T$  of  $\sigma_0$  in these materials.<sup>1-5</sup> Nevertheless, we have used Eqs. (1)-(4) to compute  $R_S - R_N$  for a variety of parameters. Two examples are shown in Fig. 4(a). The upper curve shows the case where essentially all the material becomes superconducting; in the lower curve  $\frac{1}{2}$  remains normal. Comparison of these curves with each other shows that both the maximum and the zero crossing are sensitive to the value of  $f$ . A scaling of these particular curves onto the data [shown in absolute frequency

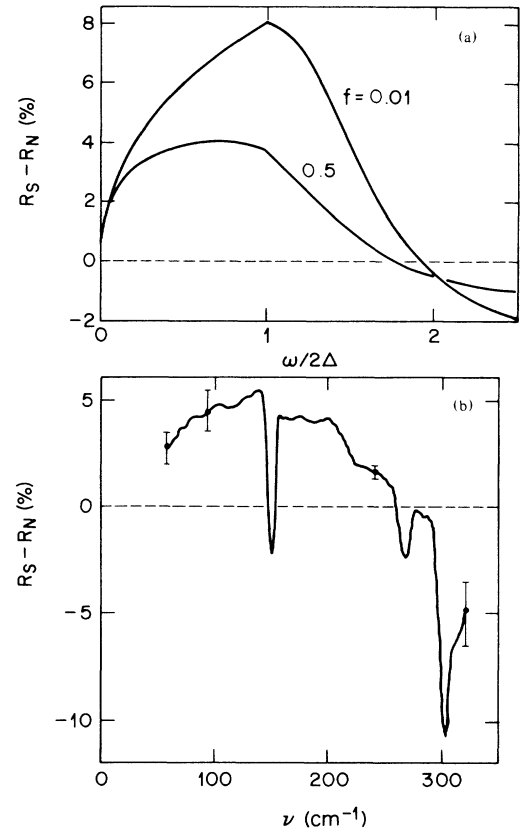


FIG. 4. (a) Theoretical superconducting-normal reflectivity difference,  $R_S - R_N$ , as a function of normalized frequency within effective medium theory for nonsuperconducting fractions  $f=0.01$  (essentially as in Fig. 3) and  $f=0.5$  (half normal in the surface region probed experimentally); (b) experimental reflectivity difference as a function of absolute frequency for same sample as in Fig. 2.

units in Fig. 4(b)] leads to estimates of the ratio  $r$  of the optical gap to  $T_c$ ,  $r \equiv 2\Delta/k_B T_c$ , of 2.3 (for  $f=0$ ) and 3.5 (for  $f=0.5$ ). The  $r$  predicted by BCS theory is 3.5, which would put  $2\Delta$  at  $228 \text{ cm}^{-1}$ . This analysis applies in a similar way to the  $(\text{La,Sr})_2\text{CuO}_4$  data.<sup>10-14</sup>

The data in Fig. 2 clearly show  $f > 0$  and therefore argue against the theoretical comparison in Fig. 4 that leads to  $r \sim 2.3$ . Within our crude model,  $f \sim 0.5$  provides a reasonable description of  $R_S - R_N$  and therefore suggests  $r \sim 3.5$ . But, given the dependence of the results on the choice of  $f$ , as well as our simplification of only considering the effective medium aspect of the problem, this estimate must be regarded as provisional.

The only tunneling measurements which we are aware of on the nominally single phase material<sup>8</sup> give  $r$  of 4.8, but the composition of the grain into which the tunneling was carried out is unknown. The difference between tunneling and optical results may occur because the far-infrared beam averages over a volume that is of order  $10 \mu\text{m}$  thick and up to  $\sim 10 \text{ mm}^2$  in area, as well as over a region of  $k$  space, whereas tunneling probes a much smaller region (in both real and  $k$  space) that is selected experi-

mentally and is not necessarily typical. Other measurements<sup>9</sup> on mixed-phase material give different results.

Since the Drude fit to  $R_N$  is not good, we have tested adding an oscillator of large spectral weight to the dielectric function at energies above those studied here. In this case, there would be a large positive contribution to the real part of the dielectric function in our frequency range, and our fits indicate that the zero crossing in  $R_S - R_N$  could lie below  $2\Delta$ , yielding  $r$  above 3.5. This modeling as well as that summarized in Fig. 4, gives a spectrum within the framework of BCS theory that is qualitatively similar to the experimental curve.

Clearly, further experimental and theoretical work is needed and a definitive analysis may hinge on measurements of well characterized single crystals if the material has significant anisotropy. Nevertheless, our measurements and analysis at this stage appear to favor theoretical models for the origin of the superconductivity which produce a far-infrared spectrum similar to that of the BCS pairing model.

We would like to thank G. Musser for technical assistance, and B. Batlogg, J. Orenstein, C. M. Varma, and W. Weber for helpful discussions.

\*Permanent address: Department of Physics, Florida State University, Tallahassee, FL.

<sup>1</sup>M. K. Wu, J. R. Ashburn, C. J. Torng, P. H. Hor, R. L. Meng, L. Gao, Z. J. Huang, Y. Q. Wang, and C. W. Chu, Phys. Rev. Lett. **58**, 908 (1987).

<sup>2</sup>J. M. Tarascon, L. R. Greene, W. R. McKinnon, and G. W. Hull, Phys. Rev. B **35**, 7115 (1987).

<sup>3</sup>R. J. Cava, B. Batlogg, R. B. van Dover, D. W. Murphy, S. Sunshine, T. Siegrist, J. P. Remeika, E. A. Rietman, S. Zahurak, and G. P. Espinosa, Phys. Rev. Lett. **58**, 1676 (1987).

<sup>4</sup>Y. LePage, W. R. McKinnon, J. M. Tarascon, L. H. Greene, G. W. Hull, and D. Hwang, Phys. Rev. B **35**, 7245 (1987).

<sup>5</sup>P. Ganguly, R. A. Mohan Ram, K. Sreedhar, and C. N. R. Rao, Pramana **28**, L321 (1987); C. N. R. Rao, P. Ganguly, A. K. Raychaudhuri, K. A. Mohan, and K. Sreedhar, Nature (London) **326**, 638 (1987).

<sup>6</sup>D. C. Mattis and J. Bardeen, Phys. Rev. **111**, 412 (1958).

<sup>7</sup>See, for example, D. A. G. Bruggeman, Ann. Phys. (Leipzig) **24**, 636 (1935).

<sup>8</sup>J. Moreland, J. W. Ekin, L. F. Goodrich, T. E. Capobianco, A. F. Clark, J. R. Kwo, M. Hong, and S. H. Liou, Phys. Rev. B **35**, 8856 (1987).

<sup>9</sup>J. R. Kirtley, W. J. Gallagher, Z. Schlesinger, R. L. Sandstrom, T. R. Dinger, and D. A. Chance, Phys. Rev. B **35**, 8846 (1987).

<sup>10</sup>P. E. Sulewski, A. J. Sievers, S. E. Russek, H. D. Mallen, D. K. Lathrop, and R. A. Buhrman, Phys. Rev. B **35**, 5330 (1987); P. E. Sulewski, A. J. Sievers, R. A. Buhrman, J. M. Tarascon, and L. H. Greene, *ibid.* **35**, 8829 (1987).

<sup>11</sup>D. A. Bonn, J. E. Greedan, C. V. Stager, and T. Timusk, Solid State Commun. (to be published).

<sup>12</sup>U. Walter, M. S. Sherwin, A. Stacy, P. L. Richards, and A. Zettl, Phys. Rev. B **35**, 5327 (1987).

<sup>13</sup>Z. Schlesinger, R. L. Greene, J. G. Bednorz, and K. A. Müller, Phys. Rev. B **35**, 5334 (1987); Z. Schlesinger, R. T. Collins and M. W. Shafer, *ibid.* **35**, 7232 (1987).

<sup>14</sup>G. A. Thomas, A. J. Millis, R. N. Bhatt, R. J. Cava, and E. A. Rietman, this issue, Phys. Rev. B **36**, 736 (1987).

<sup>15</sup>T. Ekino, J. Akimitsu, M. Sato, and S. Hosoya, Solid State Commun. (to be published).

<sup>16</sup>See, e.g., M. E. Hawley, K. E. Gray, D. W. Capone II, and D. G. Hinks, Phys. Rev. B **35**, 7224 (1987); J. R. Kirtley, C. C. Tsuei, S. I. Park, C. C. Chi, J. Rozen, and M. W. Shafer, *ibid.* **35**, 7216 (1987).

<sup>17</sup>W. Weber, Phys. Rev. Lett. **58**, 1371 (1987).